

A revised geochronology of Thurston Island, West Antarctica and correlations along the proto-Pacific margin of Gondwana

T.R. Riley¹, M.J. Flowerdew^{1,2}, R.J. Pankhurst³, P.T. Leat^{1,4}, I.L. Millar³, C.M. Fanning⁵ & M.J. Whitehouse⁶

¹*British Antarctic Survey, High Cross, Madingley Road, Cambridge, CB3 0ET, UK*

²*CASP, 181A Huntingdon Road, Cambridge, CB3 0DH, UK*

³*British Geological Survey, Keyworth, Nottingham, NG12 5GG, UK*

⁴*Department of Geology, University of Leicester, Leicester, LE1 7RH, UK*

⁵*Research School of Earth Sciences, The Australian National University, Canberra ACT 0200, Australia*

⁶*Swedish Museum of Natural History, Box 50007, SE-104 05 Stockholm, Sweden*

*Author for correspondence

e-mail: trr@bas.ac.uk

Tel. 44 (0) 1223 221423

Abstract

The continental margin of Gondwana preserves a record of long-lived magmatism from the Andean Cordillera to Australia. The crustal blocks of West Antarctica form part of this margin, with Palaeozoic – Mesozoic magmatism particularly well preserved in the Antarctic Peninsula and Marie Byrd Land. Magmatic events on the intervening Thurston Island crustal block are poorly defined, which has hindered accurate correlations along the margin. Six samples are dated here using U-Pb geochronology and cover the geological history on Thurston Island. The basement gneisses from Morgan Inlet have a protolith age of 349 ± 2 Ma and correlate closely with the Devonian – Carboniferous magmatism of Marie Byrd Land and New Zealand. Triassic (240 – 220 Ma) magmatism is identified at two sites on Thurston Island, with Hf isotopes indicating magma extraction from Mesoproterozoic-age lower crust. Several sites on Thurston Island preserve rhyolitic tuffs that have been dated at 182 Ma and are likely to correlate with the successions in the Antarctic Peninsula, particularly given the pre-break-up position of the Thurston Island crustal block. Silicic volcanism was widespread in Patagonia and the Antarctic Peninsula at ~183 Ma forming the extensive Chon Aike Province. The most extensive episode of magmatism along the active margin took place during the mid-Cretaceous. This Cordillera ‘flare-up’ event of the Gondwana margin is also developed on Thurston Island with granitoid magmatism dated in the interval 110 – 100 Ma.

Keywords: Geochronology, zircon, Hf isotopes, Marie Byrd Land, granite, volcanic

Introduction

West Antarctica consists of five major and geologically distinctive crustal blocks (Storey et al. 1988), which formed part of the Palaeozoic and Mesozoic continental margin of Gondwana (Fig. 1).

The Thurston Island and Marie Byrd Land crustal blocks have geological histories that, in many respects, resemble that of the adjacent Antarctic Peninsula crustal block (Fig. 1). However in other respects their geological histories more closely resemble that recorded in parts of New Zealand (e.g. Korhonen et al. 2010), which was formerly situated outboard of Marie Byrd Land, prior to Gondwana break-up (Yakymchuk et al. 2015). The relative position of the crustal blocks of West Antarctica and any geological relationships between them remain poorly understood (e.g. Veevers, 2012), largely as a result of the absence of reliable geochronology on key units, particularly on Thurston Island.

Palaeozoic and Mesozoic magmatic arc rocks in the Antarctic Peninsula, Thurston Island and Marie Byrd Land preserve an important record of subduction before, during and after Gondwana break-up (e.g. Leat et al. 1993). Recent geochemical and geochronological research from the Antarctic Peninsula (Millar et al. 2001, 2002; Riley et al. 2012; Vaughan et al. 2012) and from Marie Byrd Land (Mukasa & Dalziel 2000; Korhonen et al. 2010; Yakymchuk et al. 2015) have allowed an improved understanding of their geological histories and how they are related. The geochemistry and geochronology of Thurston Island magmatism has been documented by Leat et al. (1993) and Pankhurst et al. (1993) respectively. The geochronology presented by Pankhurst et al. (1993) was based on whole rock and mineral $^{40}\text{Ar}/^{39}\text{Ar}$, K-Ar and Rb-Sr dating, which are not as reliable for dating magmatic events as U-Pb zircon data recently used from the Antarctic Peninsula and Marie Byrd Land.

This paper presents new U-Pb geochronology from Thurston Island and includes samples from the main known magmatic units. The results are compared with the previous geochronology (Pankhurst et al. 1993) and the implications of these on correlations along the proto-Pacific margin of Gondwana are discussed.

Geological background and previous geochronology

Thurston Island is 240 km long and up to 100 km in width (Fig. 2a); any rock exposure is limited and geological contacts are rare. The geology of Thurston Island, its associated minor islands, the adjacent Eights Coast and Jones Mountains (Fig. 2a) have previously been described by Craddock et al. (1969), Craddock (1972), Lopatin & Orlenko (1972), Rowley (1990), Storey et al. (1991), Leat et al. (1993), Pankhurst et al. (1993) and Kipf et al. (2012).

Thurston Island and the adjacent mainland that forms the crustal block consists of a basement sequence of variably tectonised calc-alkaline igneous rocks recording Pacific-margin magmatism of Carboniferous to Late Cretaceous age (White & Craddock 1987; Leat et al. 1993; Pankhurst et al. 1993; Kipf et al., 2012). These magmatic rocks are overlain, in places, by Miocene alkali basalts, which were erupted following the cessation of subduction along this margin. Pankhurst et al. (1993) divided the basement geology of Thurston Island into seven groups on the basis of field relationships and geochronology. Their groups were (1) Late Carboniferous granitic basement; (2) Late Palaeozoic/Early Mesozoic gabbro-diorite magmatism; (3) Early Jurassic granite magmatism; (4) Jurassic (?) volcanism; (5) Late Jurassic granite magmatism; (6) Early Cretaceous gabbro-granite magmatism; (7) Mid to Late Cretaceous magmatism.

Late Carboniferous granitic basement

Craddock (1972) suggested that the whole of Thurston Island is underlain by medium- to high-grade metamorphic rocks of pre-Jurassic age, although Lopatin & Orlenko (1972) suggested a more restricted area of basement gneiss. Field observations described by Pankhurst et al. (1993) indicate that the basement gneisses occur in eastern Thurston Island in the vicinity of Morgan Inlet and Cape Menzel (Fig. 2b). The primary lithology is a granodiorite-leucogranite gneiss unit and was interpreted

by Leat et al. (1993) to be part of an ensialic magmatic arc. The magmatic protolith at Morgan Inlet was dated by whole rock Rb-Sr at 309 ± 5 Ma (Pankhurst et al. 1993).

Late Palaeozoic/Early Mesozoic mafic magmatism

The gabbro/diorite intrusive rocks, which were identified as a separate group by Lopatin & Orlenko (1972) crop out in the northern part of central and eastern Thurston Island. The primary lithology is hornblende gabbro, which is typically medium-grained and undeformed. Pankhurst et al. (1993) had difficulty dating the gabbros with K-Ar (hornblende and biotite) and $^{40}\text{Ar}/^{39}\text{Ar}$ (biotite) yielding ages in the range (240 – 220 Ma), but in view of the pristine igneous nature of these rocks and absences of subsequent deformation or metamorphism, they concluded that crystallization was approximately 237 ± 6 Ma.

Early Jurassic granites

Coarsely crystalline, porphyritic pink granites crop out at the adjacent Jones Mountains on the mainland (Fig. 2a) beneath a Cenozoic unconformity and were dated by Pankhurst et al. (1993) using whole rock Rb-Sr (198 ± 2 Ma), although a muscovite separate yielded a younger K-Ar age of 183 ± 5 Ma.

Jurassic volcanism

The Jurassic volcanic rocks of Thurston Island are calc-alkaline lavas and pyroclastic rocks that vary in composition from basalt to rhyolite. Pankhurst et al. (1993) encountered difficulty in dating the volcanic rocks as a result of low-grade metamorphism and the extensive development of secondary minerals. Nevertheless, six samples from a sequence of andesitic tuffs and banded rhyolite flows at Mount Dowling (Fig. 2b) yielded a whole rock Rb-Sr errorchron with an age of 164 ± 9 Ma. A separate felsite unit gave a considerably older Rb-Sr whole rock age of 182 ± 2 Ma.

Basaltic – rhyolitic volcanic rocks are also reported from the Jones Mountains, but no age information exists.

Late Jurassic granite magmatism

The western and southern parts of Thurston Island are largely composed of homogeneous, pink porphyritic granites (White & Craddock 1987) and they represent the most widespread magmatic event on Thurston Island.

Pankhurst et al. (1993) dated several granitic plutons using Rb-Sr, K-Ar and $^{40}\text{Ar}/^{39}\text{Ar}$ techniques. They identified ages in the range 153 – 138 Ma, with a peak at c. 144 Ma. The plutons are granite – granodiorite in composition, with rare, more dioritic compositions (Leat et al. 1993).

Early Cretaceous gabbro – granite magmatism

Eastern Thurston Island and the adjacent islands of the Eights Coast (Fig. 2a) are characterised by rocks that are typically more mafic than those exposed in the west (White & Craddock 1987). They are gabbro – diorite in composition and were dated by Pankhurst et al. (1993) using Rb-Sr and K-Ar (biotite) methods and typically yielded ages in the range 127 – 121 Ma, although biotite from a gabbro at Dustin Island (Fig. 2b) yielded a younger age of 110 Ma, which was taken to mark the final stage of Early Cretaceous magmatism on Thurston Island.

Mid to Late Cretaceous magmatism

A separate, identifiable magmatic episode is exposed in the Jones Mountains, where dominantly felsic (dacite – rhyolite) lavas and tuffs crop out, along with associated mafic – silicic dykes (Leat et al. 1993). Three separate suites of samples were dated by Pankhurst et al. (1993) using Rb-Sr (whole rock). Their results were variable, but yielded ages in the range 102 – 89 Ma although Pankhurst et al. (1993) urged caution in their reliability and suspected Rb-Sr systems may have been reset.

Geochronology and Hf isotope geochemistry

This study

Six samples were selected from the Thurston Island crustal block in an attempt to represent the broad range of magmatic rocks and events that are exposed across the region. The selected samples should permit robust correlations to be made with the neighbouring crustal blocks of West Antarctica and further along the proto-Pacific margin of Gondwana.

Analytical techniques

U-Pb geochronology was carried out using the Cameca IMS 1280 ion microprobe, housed at the NORDSIM isotope facility, Swedish Museum of Natural History (Stockholm) and the Sensitive High Resolution Ion Microprobe (SHRIMP) at the Australian National University, Canberra.

Zircons, separated by standard heavy liquid procedures, were mounted in epoxy and polished to expose their interiors. They were imaged by optical microscopy and cathodo-luminescence (CL) prior to analysis. The CL images were used as guides for analysis targets because they reveal the internal structure of the grains. The analytical methods using the NORDSIM facility closely followed those detailed by Whitehouse & Kamber (2005). U/Pb ratio calibration was based on analysis of the Geostandard reference zircon 91500, which has a $^{206}\text{Pb}/^{238}\text{U}$ age of 1065.4 ± 0.6 Ma and U and Pb concentrations of 81 and 15 ppm respectively (Wiedenbeck et al. 1995). At the SHRIMP facility the analytical method followed that outlined by Williams (1998). Calibration was carried out using zircon standards mounted together with the samples (mostly AS-3; Paces & Miller 1993).

Common lead corrections were applied using a modern day average terrestrial common lead composition ($^{207}\text{Pb}/^{206}\text{Pb} = 0.83$; Stacey & Kramers 1975) where significant ^{204}Pb counts were recorded. Age calculations were made using Isoplot v.3.1 (Ludwig 2003) and the calculation of concordia ages followed the procedure of Ludwig (1998). The results are summarised in Table 1.

Hf isotopic determinations were made using a 266nm Merchantek Nd:YAG laser attached to a VG Axiom multi-collector inductively coupled mass spectrometer at the NERC Isotope Geosciences Laboratory, UK. Analyses were carried out, where possible, on top of the original ion-microprobe-generated pit, so that Hf analysis could be paired with different stages of zircon growth. Where it was not possible to do so, CL images were used to identify areas of zircon interpreted to have the same age. The Hf analytical method follows that described by Flowerdew et al. (2006). Repeat analysis of 91500 monitor standard yielded $^{176}\text{Hf}/^{177}\text{Hf}$ 0.282300 ± 77 ($n = 32$). The results are summarised in Table 2.

Morgan Inlet

Sample R.3035.3 is a granodiorite gneiss from Morgan Inlet (Fig. 2b) and is considered to be from the oldest exposed magmatic unit on Thurston Island. Pankhurst et al. (1993) recorded a Rb-Sr whole rock age of 309 ± 5 Ma (MSWD 3.4, initial $^{87}\text{Sr}/^{86}\text{Sr}$: 0.7040) for a series of gneiss samples including sample R.3035.3.

R.3035.3 contains large (200 – 500 μm), stubby, but prismatic (aspect ratio typically 2:1) grains. Under cathodo-luminescence (CL) a complex zircon internal structure is apparent (Supplementary Fig. 1). Most zircons comprise an inner portion displaying fine-scale growth typical of crystallisation from a magma during intrusion, but also a ubiquitous, thin outer (typically 30 μm) zone which cuts across growth zones of the inner portion. The CL character of the outer portion is also different, with a gradient from strongly to weakly luminescent from the zircon inner zone to the rim.

Twenty eight analyses of zircon grains (Table 1) include one that has lost radiogenic Pb (318 Ma) and four older ages that are interpreted to represent pre-Carboniferous inherited zircon (1019 – 386 Ma). The remaining $^{206}\text{Pb}/^{238}\text{U}$ ages range from range from 365 to 331 Ma with a weighted mean of 347 ± 4 Ma, but outside analytical error as indicated by an MSWD of 3.3 and it is notable that the two analyses of the thin outer zircon phase give ages indistinguishable from those of the inner core. This range could be attributed either to minor Pb-loss at the younger end due to the effects of

penecontemporaneous metamorphism or to inheritance of a precursor magmatic phase at 365–360 Ma, or indeed to both effects. On this basis, 15 ages give a weighted mean of 349 ± 2 Ma with a MSWD of 1.1, and this is taken as best representing the crystallization age of the granitoid protolith (Fig. 3a).

Nineteen Hf isotopic analyses on the 349 Ma portions from 17 grains yield positive ϵ_{Hf} values which range between 1.0 ± 2.1 and 9.8 ± 1.2 , and a weighted average of 6.2 ± 1.2 (Fig. 4), which corresponds to a depleted mantle model age of c. 700 Ma. This indicates that the gneisses, although modestly juvenile (as indicated by the low $^{87}\text{Sr}/^{86}\text{Sr}_i$ ratio and low ϵ_{Nd_i} values of -0.7 to +2.1; Pankhurst et al. 1993) had involved some older crust during petrogenesis, consistent with the minor occurrence of inherited zircons of Early Palaeozoic and Proterozoic age.

Mount Bramhall

Medium grained, weakly deformed, diorite/granodiorite from Mount Bramhall (Fig. 2b) previously yielded hornblende (K-Ar) and biotite (K-Ar, $^{40}\text{Ar}/^{39}\text{Ar}$, Rb-Sr) mineral cooling ages of 237 ± 6 Ma and c. 228 Ma, respectively (Pankhurst et al. 1993).

Sample R.3031.1 is a diorite from Mount Bramhall and is the same sample which yielded a 225 ± 6 Ma K-Ar biotite cooling age reported by Pankhurst et al. (1993). Separated zircons are typically 200 μm prisms with aspect ratios of 3:1 (Supplementary Fig. 1). The internal structure is generally simple with growth zoning often with a less luminescent outer zone. Rare zircon cores are rounded and have a CL character that is different from the surrounding rim. Five analyses from zircons with the growth zoned texture yield a weighted mean of the $^{206}\text{Pb}/^{238}\text{U}$ ages of 239 ± 4 Ma with a MSWD of 1.9 (Fig. 3a), which is considered to date the intrusion and is consistent with the K-Ar hornblende age reported by Pankhurst et al. (1993). Inherited cores have $^{206}\text{Pb}/^{238}\text{U}$ ages of 411 ± 8 , 611 ± 12 and 961 ± 18 Ma.

Seven Hf isotope analyses from portions of 5 separate c. 239 Ma grains yield ϵ_{Hf} values which range between 0.3 ± 3.7 and 7.6 ± 4.0 . The average of the analyses of -2.6 ± 2.5 (Fig. 4), which

corresponds to a depleted mantle model age of c. 950 Ma, indicates that older crust was involved in the petrogenesis of the diorite, consistent with initial $^{87}\text{Sr}/^{86}\text{Sr}$ ratios of ~ 0.7067 and negative ϵNd_i of c. -3.7 (Pankhurst et al. 1993).

Mount Dowling

Zircons were separated from two of the volcanic rock samples which yielded a 164 ± 9 Ma whole rock Rb-Sr age (Pankhurst et al. 1993). R.3029.1 is a crystal lithic tuff and sample R.3029.3 is a fine grained crystal tuff. Both rocks are rhyolitic in composition and are characterised by embayed quartz grains. Zircons from both samples have similar characteristics typical of felsic volcanic rocks; they are small ($<100 \mu\text{m}$), prismatic (5:1 ratio) and have CL characteristics (Supplementary Fig. 1) that are consistent with having crystallised from a magma (Corfu et al. 2003).

Sample R.3029.1 yields a weighted mean of the $^{206}\text{Pb}/^{238}\text{U}$ ages of 181 ± 1 Ma with a MSWD of 0.9 when analysis 2, interpreted to have suffered recent Pb loss, is excluded from the age calculation (Fig. 3b). Textural evidence for older inherited zircons as is evident from cores in the CL images (Supplementary Fig. 1) and these cores are older, yielding ages at ~ 350 , 980 and 2460 Ma. Sample R.3029.3 yields an indistinguishable age to R.3029.1 of 182 ± 1 Ma with a MSWD of 1.0 and lacks discernible inheritance in the CL images (Supplementary Fig) nor any evidence from the ages obtained from the individual zircon grains.

Hale Glacier

Pankhurst et al. (1993) dated a megacrystic, pink, biotite granite from the Hale Glacier area, which gave a Rb-Sr whole rock age of 142 ± 5 Ma, which is in agreement with their K-Ar biotite cooling age of 144 ± 4 Ma. The Hale Glacier granite is part of the Late Jurassic/Early Cretaceous granite magmatism of Pankhurst et al. (1993).

Sample R.3025.3 from Hale Glacier is dated here and is a pink, megacrystic biotite granite. Zircons are typically 200-300 μm prisms with 3:1 aspect ratios and display diffuse growth and sector zoning

under CL, textures which are typical of crystallisation in granitoid magmas. Zircon inheritance was not evident from the CL images (Supplementary Fig. 1). Eight analyses from eight grains yields a weighted mean of the $^{206}\text{Pb}/^{238}\text{U}$ ages 151 ± 2 Ma with a MSWD of concordance of 2.4 (Fig. 3c).

Seven hafnium isotopic analyses from 3 grains yield ϵHf_i values that range between -7.9 ± 3.5 and 2.6 ± 2.2 (Fig. 4). The resulting average of -2.4 ± 2.6 corresponds to a depleted mantle model age of 860 Ma, and indicates that some older crust was involved in the petrogenesis of the Hale Glacier granite.

Lepley Nunatak

Lepley Nunatak is the easternmost exposure on the Eights Coast (Fig. 2a) and is characterised by calcic granodiorite and coarsely crystalline, biotite granite. These rocks have yielded $^{40}\text{Ar}/^{39}\text{Ar}$ and K-Ar biotite ages of 89 ± 1 Ma and 87 ± 2 Ma, respectively (Pankhurst et al. 1993).

Sample R.3032.4 is biotite granite and was selected for U-Pb analysis. Zircons are typically 200 μm squat prisms with fine-scale growth and diffuse sector zoning under CL (Supplementary Fig. 1) and also display textural evidence for inherited grains preserved as irregular CL-dark cores. Seven analyses from the growth-zoned portions of seven separate grains yields a weighted mean of the $^{206}\text{Pb}/^{238}\text{U}$ ages of 108 ± 1 Ma with a MSWD of 2.2 (Fig. 3c), which is interpreted to date the intrusion.

Eight hafnium isotopic analyses from the c. 108 Ma portions of 3 zircons yield ϵHf_i values which range between -8.8 ± 3.5 and -1.2 ± 2.3 . An average ϵHf_i of -2.9 ± 2.0 (Fig. 4) and depleted mantle model age of 860 Ma confirms involvement of old rocks in their petrogenesis, and was indicated by the numerous inherited zircons in this sample.

Revised chronology of Thurston Island, correlations along the Gondwana margin and Hf isotopes

Following the U-Pb geochronology carried out as part of this study, the following revisions can be made to the tectonic and magmatic evolution of the Thurston Island crustal block.

Devonian – Carboniferous magmatism

New data presented here has significantly revised the geological development of Thurston Island. The similarity in age between the c. 349 Ma granodioritic orthogneiss at Morgan Inlet and granodioritic rocks from western Marie Byrd Land (Fig. 1) suggest that they may be correlatives. Korhonen et al. (2010) dated several granitoids from the Fosdick Mountains area (Marie Byrd Land; Fig. 1) that yielded Carboniferous ages of 358 ± 8 , 350 ± 10 , 343 ± 8 Ma and also dated Cretaceous-age magmatism with zircon cores of c. 355 Ma. Korhonen et al. (2010) interpreted the c. 350 Ma Carboniferous event to be the result of partial melting of the Devonian (c. 375 Ma) Ford granodiorite suite.

Yakymchuk et al. (2015) reported a broader range of ages for the Ford Granodiorite suite (375 – 345 Ma), but with two distinct magmatic episodes. An older suite (c. 370 Ma) was interpreted to be the result of mixing of a juvenile magma with metaturbidites of the Swanson Formation, whilst the younger suite (c. 350 Ma), which overlaps in age with the Morgan Inlet gneisses, were interpreted to have a greater contribution from paragneisses of the Swanson Formation or anatexis of the Ford granodiorite suite (Korhonen et al. 2010).

The ϵHf_i data of the c. 350 Ma granodiorites from the Ford Ranges of Marie Byrd Land is in the range +2 to -5 (Yakymchuk et al. 2015), whereas the granodioritic gneiss from Thurston Island has ϵHf_i in the range +10 to +2 (Fig. 4). This discrepancy suggests that the Thurston Island magmatism was considerably more juvenile than that in western Marie Byrd Land. The values from the Morgan Inlet gneisses are, however, in close agreement with those obtained from New Zealand where c. 350 Ma magmatic zircons yielded ϵHf_i values of +7 to +2 (Scott et al. 2009; Fig. 4).

Early Carboniferous magmatism or metamorphism has not been recognised on the adjacent Antarctic Peninsula (Riley et al. 2012). There is a minor metamorphic event at c. 330 Ma (Millar et al.

2002), but Riley et al. (2012) demonstrated that this event was likely to have been restricted to the northern Antarctic Peninsula, although it potentially may coincide with a more widespread event (346 ± 4 Ma) in the Deseado Massif of southern Patagonia (Pankhurst et al. 2003).

Triassic magmatism

The U-Pb results presented here date granitoid (diorite/granodiorite) magmatism at Mount Bramhall (Fig. 2b) at 239 ± 4 Ma. This magmatism is potentially part of a Triassic event that is widely exposed across the southern Antarctic Peninsula (Palmer Land). Millar et al. (2002) published magmatic and metamorphic ages from Campbell Ridge, Mount Eissenger, Pegasus Mountains and Sirius Cliffs (Fig. 1) that fall in the age range 230 – 220 Ma. Riley et al. (2012) and Flowerdew et al. (2006) also reported widespread Triassic magmatism and metamorphism in the Joerg Peninsula (Fig. 1) area of Graham Land (236 ± 2 and 224 ± 4 Ma).

Triassic magmatism is known from the Kohler Range and Mount Isherwood in the Walgreen Coast (Fig. 1), i.e. the adjacent part of Marie Byrd Land to Thurston Island (Pankhurst et al. 1998; Mukasa and Dalziel 2000). Korhonen et al. (2010) also document inherited, small ($<200 \mu\text{m}$) Triassic zircons from Cretaceous-age granitoids in Marie Byrd Land. Indirect evidence for Triassic magmatism is widespread in New Zealand as metasedimentary rocks within numerous terranes contain abundant c. 240 Ma detrital zircons (e.g. Adams et al. 2008; Scott et al. 2009; Wysoczanski et al 1997). Triassic (and late Permian) granite-rhyolite magmatism is also widespread in northern Patagonia (e.g., Pankhurst et al. 2006).

Jurassic magmatism

Silicic tuffs from Mount Dowling (Fig. 2b) have been dated here at 182 – 181 Ma, some 20 Myr older than the age proposed by Pankhurst et al. (1993). The new age is consistent with the ages of major Gondwana break-up magmatic events of the Chon Aike, Karoo and Ferrar provinces (Riley & Knight 2000). Elsewhere along the proto-Pacific margin in Marie Byrd Land, evidence for Early – Middle

Jurassic magmatism is limited; Korhonen et al. (2010) report just a single inherited zircon grain at 181 ± 11 Ma from a Cretaceous-age granite in the northern Fosdick Mountains (Fig. 1), but there are no reported Jurassic volcanic rocks from Marie Byrd Land, although Adams (1987) does report a Rb-Sr (biotite) age of 165 ± 2 Ma from a granite near Mount Morgan; this was considered by Adams (1987) to be a potentially reset age.

Further north along the margin, the Antarctic Peninsula has multiple occurrences of silicic volcanism at ~ 183 Ma, particularly in Palmer Land. The Mount Poster and Brennecke formations of southern Palmer Land (Fig. 1) form part of the extensive Chon Aike Province (V1 event; Pankhurst et al. 2000). The Chon Aike Province of Patagonia and the Antarctic Peninsula has been described by Pankhurst et al. (1998, 2000) who identified three distinct volcanic episodes (V1: ~ 183 Ma; V2: ~ 170 Ma; V3: ~ 155 Ma). The Mount Poster and Brennecke formations of the southern Antarctic Peninsula (Palmer Land) have been dated at 183.4 ± 1.4 Ma (Mount Poster Formation; Hunter et al. 2006) and 184.2 ± 2.5 Ma (Brennecke Formation; Pankhurst et al. 2000) and overlap in age with the Mount Dowling volcanism of Thurston Island. Lithologically, the silicic volcanism from Thurston Island is akin to the dominantly silicic tuffs and ignimbrites of Palmer Land, where associated mafic volcanism is rare (Riley et al. 2016). The age information favours a pre break-up reconstruction which places the Thurston Island crustal block in a rotated position and one where Thurston Island was juxtaposed with the southern Antarctic Peninsula (Fig. 5). Both Veevers (2012) and Elliot et al. (2016) propose a rotated position for the Thurston Island crustal block at ~ 180 Ma, although Veevers (2012) propose a 180° rotation and Elliot et al. (2016) a 90° rotation. Either rotation scenario place the Mount Dowling silicic volcanic rocks more adjacent to the silicic formations of the southern Antarctic Peninsula (Fig. 5).

Isotopically (Sr-Nd), the silicic volcanic rocks from Mount Dowling are close in composition (Fig. 6) to the rhyolitic tuffs of the Brennecke Formation (Riley et al. 2001) and also the V1 (~ 183 Ma) equivalent rhyolitic tuffs in Patagonia, the Marifil Formation (Pankhurst et al. 2000). The contemporaneous Mount Poster Formation of Palmer Land is however isotopically distinct (Fig. 6) to

all other Early Jurassic volcanic rocks of the Gondwana margin and has been attributed by Riley et al. (2001) to significant upper crustal contamination as a result of its long-lived caldera setting and is considered to be a localised petrogenetic feature.

Late Jurassic magmatism is confirmed from the Hale Glacier area (Fig. 2b), with a U-Pb age of 151 ± 2 Ma recorded here from a pink, megacrystic granite, although it is significantly older than the 142 ± 5 Ma age of Pankhurst et al. (1993). They also dated granitoids from Landfall Peak, Henderson Knob, Mount Simpson and Long Glacier (Fig. 2b), which gave Rb-Sr ages in the range 153 – 144 Ma. The Late Jurassic – Early Cretaceous granitoids crop out extensively in the western and southern parts of Thurston Island and may represent part of a compound batholith (Leat et al. 1993).

Late Jurassic magmatism on the Antarctic Peninsula is rare, with Leat et al. (1995) not reporting any granitoid magmatism from this age. However, Early Cretaceous plutonism at $\sim 141 \pm 2$ Ma is reported from northwest Palmer Land (Vaughan & Millar, 1996) and may mark the onset of a major magmatic event during the mid-Cretaceous.

Late Jurassic – Early Cretaceous magmatism is also rare in Marie Byrd Land, although along the eastern margin of the Ford Ranges (Fig. 1) a series of high level, small plutons has been dated in this period (Rb-Sr, K-Ar; Adams, 1987). Korhonen et al. (2010) record no Late Jurassic magmatism from the northern Ford Ranges area (Fig. 1) of Marie Byrd Land and identified no inherited grains from this period in the Late Cretaceous granitoids. Kipf et al. (2012) dated a granitoid from eastern Marie Byrd Land at 147.2 ± 0.4 Ma, which is adjacent to the Thurston Island crustal block. Granites in the age range 157 – 145 Ma mark the earliest stage of Andean subduction in the South Patagonian batholith, overlapping with the final stage of widespread ignimbrite eruption (Hervé et al. 2007).

The ϵHf_i isotopes from the Late Jurassic granitoids also lie on the evolution trend (Fig. 4) of the Late Mesoproterozoic Haag Nunataks gneiss (BAS unpublished data), with evolved ϵHf_i values of typically -2 to -7. The occurrence of Jurassic magmatism in the west of Thurston Island but older Triassic and Carboniferous units to the east are also consistent with the pre break-up position shown in Fig. 5. This reconstruction is consistent with a broad younging of protolith ages from the

hinterland toward the margin. It is therefore likely that rotation of the Thurston Island crustal block into its current position is constrained between the Late Jurassic and the mid-Cretaceous.

Cretaceous magmatism

Mid-Cretaceous magmatism is widespread along the entire proto-Pacific margin of Gondwana, with the period a time of global plate reorganisation and intense magmatism (Vaughan et al. 2012). This is particularly evident along the Andean Cordillera, which was marked by a major magmatic event ('flare-up') at ~110 Ma (Paterson & Ducea 2015). The U-Pb ages presented here from Lepley Nunatak on the Eights Coast of 108 ± 1 Ma is close to the range defined by Pankhurst et al. (1993) for this episode on the Thurston Island crustal block of 102 – 89 Ma and also the range defined by Kipf et al. (2012) of 110 – 95 Ma.

Magmatism arising from crustal anatexis in Marie Byrd Land was also extensive during the interval, 115 – 98 Ma (Siddoway et al. 2005; Korhonen et al. 2010; McFadden et al. 2010), which can be divided into two distinct chronological groups at 115 – 110 Ma and 109 – 102 Ma based on their geochemistry and emplacement depth. Korhonen et al. (2010) interpreted the older episode to be derived from the Carboniferous Ford granodiorite suite, whilst the younger magmatic episode was compositionally more closely related to the pre-Devonian metasedimentary Swanson Formation (Yakymchuk et al. 2013, 2015).

Mid-Cretaceous magmatism on the Antarctic Peninsula is also extensive (Leat et al. 1995; Flowerdew et al. 2005), particularly during the emplacement of the Lassiter Coast Intrusive Suite (Pankhurst & Rowley 1991). The Lassiter Coast intrusive suite is an extensive suite of mafic to felsic calc-alkaline plutons exposed in southeast Palmer Land (Fig. 1). An age range of 119 – 95 Ma was indicated by Vaughan et al. (2012), which is the same age range as that recorded in Marie Byrd Land. The peak of magmatic activity in the Lassiter Coast intrusive suite occurred between 105 Ma and 110 Ma and is contemporaneous with a silicic 'flare-up' event recorded in the South American Cordillera (Paterson & Ducea 2015). Flowerdew et al. (2005) suggested, on the basis of Sr-Nd isotopes, that the

granitoids of the Lassiter Coast intrusive suite have a strong lower crustal component, similar in composition to the Mesoproterozoic orthogneisses exposed in Haag Nunataks (Millar and Pankhurst, 1987). The ϵHf_i isotopes presented here (Fig. 4) also indicate an evolution trend from a crustal composition akin to Haag Nunataks gneiss. The ϵHf_i data from Marie Byrd Land are similar to those obtained from the Lepley Nunatak intrusion (Fig. 4). The Marie Byrd Land Hf isotope signature was demonstrated by Yakymchuk et al (2013) as having resulted from the mixing of juvenile magma with Palaeozoic metasedimentary and plutonic sources rather than any Palaeoproterozoic protolith.

In New Zealand, voluminous tonalite to granite post-collisional magmatism has been described by Waight et al. (1998) from the Hohonu Batholith of the Western Province. The peak emplacement age was also ~ 110 Ma, which overlaps with adjacent subduction-related magmatism along the continental margin of New Zealand. The granitoids marked a period of rapid tectonic change along the margin, with the batholiths emplaced during a period of crustal extension. Their geochemistry indicates a source in the lower crust, with melting triggered by rapid uplift and extension of previously over thickened lithosphere. Vaughan et al. (2012) reviewed mid-Cretaceous magmatism along the proto-Pacific margin of Gondwana and found considerable evidence for structural control on pluton emplacement, particularly from the Antarctic Peninsula, New Zealand and Marie Byrd Land.

Conclusions

New age data from the Thurston Island crustal block has significantly improved the chronology of magmatism and has allowed more confident correlations to be drawn to adjacent crustal elsewhere along the proto-Pacific margin of Gondwana.

1. Well defined Devonian – Carboniferous magmatism from the Gondwana margin has been identified at multiple locations in Marie Byrd Land and the Median Batholith of New Zealand. Age data from Thurston Island (349 ± 2 Ma) confirm the presence of Early Carboniferous magmatism further to the north along the continental margin.
2. Triassic magmatism known from the Antarctic Peninsula, Marie Byrd Land and New Zealand is also confirmed from Thurston Island (239 ± 4 Ma) and are interpreted as melts with a major lower crustal component with extraction from a Mesoproterozoic source similar to those exposed at Haag Nunataks.
3. Jurassic silicic volcanism from Thurston Island is accurately dated here at c. 182 Ma and is interpreted as a direct correlative unit to the c. 183 Ma Brennecke and Mount Poster formations from the southern Antarctic Peninsula, which are part of the wider Chon Aike Province V1 event exposed extensively in Patagonia and the Antarctic Peninsula.
4. The age, chemistry and location of Carboniferous – Jurassic magmatic and volcanic rocks are consistent with a pre break-up position for the Thurston Island Block which was rotated 90° (or potentially 180°) clockwise relative to its present orientation.
5. The most extensive phase of magmatism along the entire proto-Pacific margin occurred during the mid-Cretaceous, with a magmatic peak in the interval 110 – 105 Ma. Granitoid magmatism of this period, preserved as extensive batholiths, occurred from Patagonia to southeast Australia, including Thurston Island. It marks a major Cordillera 'flare-up' event characterised by high magma intrusion rates as over-thickened lithosphere was extended and potentially melted.

Acknowledgements

This study is part of the British Antarctic Survey Polar Science for Planet Earth programme, funded by the Natural Environmental Research Council. The samples were collected as part of a joint UK/USA research programme in 1989/1990 to investigate the tectonic history of West Antarctica. Kerstin Lindén and Lev Ilyinsky are thanked for their assistance at the NORDSIM facility. This is NORDSIM contribution number 459.

References

- ADAMS, C.J. 1987. Geochronology of granite terranes in the Ford Ranges, Marie Byrd Land, West Antarctica. *New Zealand Journal of Geology and Geophysics*, **30**, 51-72.
- CRADDOCK, C., WHITE, C.M. & RUTFORD, R.H. 1969. The geology of the Eights Coast. *Antarctic Journal of the United States*, **22**, 50-51.
- CRADDOCK, C. 1972. Geologic map of Antarctica, scale 1:5,000 000. *American Geographical Society*, New York.
- CORFU, F., HANCHAR, J.M., HOSKIN, P.W.O. & KINNY, P. 2003. Atlas of zircon textures. *Reviews in Mineralogy and Geochemistry*, **53**, 469-500.
- ELLIOT, D.H., FANNING, C.M. & LAUDON, T.S. 2016. The Gondwana plate margin in the Weddell Sea sector: zircon geochronology of Upper Paleozoic (mainly Permian) strata from the Ellsworth Mountains and eastern Ellsworth Land, Antarctica. *Gondwana Research*, **29**, 234-237.
- FLOWERDEW, M.J., MILLAR, I.L., CURTIS, M.L., VAUGHAN, A.P.M., HORSTWOOD, M.S.A., WHITEHOUSE, M.J. & FANNING, C.M. 2007. Combined U-Pb geochronology and Hf geochemistry of detrital zircons of early Paleozoic sedimentary rocks, Ellsworth–Whitmore Mountains block, Antarctica. *Geological Society of America Bulletin*, **119**, 275–288.
- FLOWERDEW, M.J., MILLAR, I.L., VAUGHAN, A.P.M., HORSTWOOD, M.S.A. & FANNING, C.M. 2006. The source of granitic gneisses and migmatites in the Antarctic Peninsula: a combined U-Pb SHRIMP and laser

485 ablation Hf isotope study of complex zircons. *Contributions to Mineralogy and Petrology*, **151**,
486 751–768.

487 FLOWERDEW, M.J., MILLAR, I.L., VAUGHAN, A.P.M. & PANKHURST, R.J. 2005. Age and tectonic significance
488 of the Lassiter Coast Intrusive Suite, Eastern Ellsworth Land, Antarctic Peninsula. *Antarctic*
489 *Science*, **17**, 443-452.

490 HERVÉ, F., PANKHURST, R.J., FANNING, C.M., CALDERÓN, M. & YAXLEY, G.M. 2007. The South Patagonian
491 batholith: 150 Myr of granite magmatism on a static plate margin. *Lithos*, **97**, 373-394.

492 HUNTER, M.A., RILEY, T.R., CANTRILL, D.J., FLOWERDEW, M.J. & MILLAR, I.L. 2006. A new stratigraphy for the
493 Latady Basin, Antarctic Peninsula: Part 1, Ellsworth Land Volcanic Group. *Geological Magazine*,
494 **143**, 777-796.

495 KIPF, A., MORTIMER, N., WERNER, R., GOHL, K., VANN DEN BOGGAARD, P., HAUFF, F. & HOERNLE, K. 2012.
496 Granitoids and dykes of the Pine Island Bay region, West Antarctica. *Antarctic Science*, **24**, 473-
497 484.

498 KORHONEN, F.J., SAITO, S., BROWN, M., SIDDOWAY, C.S. & DAY, J.M.D. 2010. Multiple generations of
499 granite in the Fosdick Mountains, Marie Byrd Land, West Antarctica: implications for polyphase
500 intracrustal differentiation in a continental margin setting. *Journal of Petrology*, **51**, 627-670.

501 LEAT, P.T., STOREY, B.C. & PANKHURST, R.J. 1993. Geochemistry of Palaeozoic – Mesozoic Pacific rim
502 orogenic magmatism, Thurston Island area, West Antarctica. *Antarctic Science*, **5**, 281-296.

503 LEAT, P.T., SCARROW, J.H. & MILLAR, I.L. 1995. On the Antarctic Peninsula batholith. *Geological*
504 *Magazine*, **132**, 399-412.

505 LOPATIN, B.G. & ORLENKO, E.M. 1972. Outline of the geology of Marie Byrd Land and the Eights Coast.
506 In ADIE, R.J. ed. *Antarctic Geology and Geophysics*. Oslo: Universitetsforlaget, 245-250.

507 LUDWIG, K.R. 1998. On the treatment of concordant uranium-lead ages. *Geochimica et Cosmochimica*
508 *Acta*, **62**, 665-676.

509 LUDWIG, K.R. 2003. User manual for isoplot 3.00: a geochronological toolkit for Microsoft Excel.
510 Berkeley Geochronology Centre Special Publications 4, 1-70.

511 MCFADDEN, R.R., SIDDOWAY, C.S., TEYSSIER, C. & FANNING, C.M. 2010. Cretaceous oblique extensional
512 deformation and magma accumulation in the Fosdick Mountains migmatite-cored gneiss dome,
513 West Antarctica. *Tectonics*, 29, doi. 10.1029/2009TC002492.

514 MILLAR, I.L. & PANKHURST, R.J. 1987. Rb-Sr geochronology of the region between the Antarctic
515 Peninsula and the Transantarctic Mountains: Haag Nunataks and Mesozoic Granitoids. *In*
516 MACKENZIE, G., ed. *Gondwana Six: Structure, Tectonics and Geophysics*. Geophysical Monograph
517 No 40, American Geophysical Union, Washington, 151-160.

518 MILLAR, I.L., PANKHURST, R.J. & FANNING, C.M. 2002. Basement chronology and the Antarctic Peninsula:
519 recurrent magmatism and anatexis in the Palaeozoic Gondwana Margin. *Journal of the Geological*
520 *Society, London* **159**, 145-158.

521 MILLAR I.L., WILLAN, R.C.R., WAREHAM, C.D. & BOYCE, A.J. 2001. The role of crustal and mantle sources in
522 the genesis of granitoids of the Antarctic Peninsula and adjacent crustal blocks. *Journal of the*
523 *Geological Society, London* **158**, 855-868.

524 MUKASA, S.B. & DALZIEL, I.W.D., 2000. Marie Byrd Land, West Antarctica; evolution of Gondwana's
525 Pacific margin constrained by zircon U-Pb geochronology and feldspar common-Pb isotopic
526 compositions. *Geol. Soc. Am. Bull.* **112**, 611–627.

527 PACES, J.B. & MILLER, J.D. 1993. Precise U-Pb ages of Duluth Complex and related mafic intrusions,
528 northeastern Minnesota: Geochronological insights to physical, petrogenetic, paleomagnetic, and
529 tectonomagmatic process associated with the 1.1 Ga Midcontinent Rift System. *Journal of*
530 *Geophysical Research-Solid Earth*, **98B**, 13,997-14,013.

531 PANKHURST, R.J. & ROWLEY, P.D. 1991. Rb-Sr study of Cretaceous plutons from southern Antarctic
532 Peninsula and eastern Ellsworth Land, Antarctica. *In* THOMSON, M.R.A, CRAME, J.A. & THOMSON, J.W.
533 eds. *Geological evolution of Antarctica*. Cambridge University Press, Cambridge, 387-394.

534 PANKHURST, R.J., MILLAR, I.L., GRUNOW, A.M. & STOREY, B.C. 1993. The pre-Cenozoic magmatic history of
535 the Thurston Island crustal block, West Antarctica. *Journal of Geophysical Research*, **98** (B7),
536 11835-11849.

537 PANKHURST, R.J., LEAT, P.T., SRUOGA, P., RAPELA, C.W., MÁRQUEZ, M., STOREY, B.C. & RILEY, T.R. 1998. The
538 Chon-Aike silicic igneous province of Patagonia and related rocks in Antarctica: a silicic large
539 igneous province. *Journal of Volcanology and Geothermal Research*, **81**, 113-136.

540 PANKHURST, R.J., RILEY, T.R., FANNING, C.M. & KELLEY, S.P. 2000. Episodic silicic volcanism in Patagonia
541 and the Antarctic Peninsula: chronology of magmatism associated with break-up of Gondwana.
542 *Journal of Petrology*, **41**, 605-625.

543 PANKHURST, R.J., RAPELA, C.W., LOSKE, W.P., MARQUEZ, M. & FANNING, C.M. 2003. Chronological study of
544 the pre-Permian basement rocks of southern Patagonia. *Journal of South American Earth Sciences*
545 **16**, 27-44.

546 PANKHURST, R.J., RAPELA, C.W., FANNING, C.M. & MÁRQUEZ, M. 2006. Gondwanide continental collision
547 and the origin of Patagonia. *Earth-Science Reviews*, **76**, 235-257.

548 PATERSON, S.R. & DUCEA, M.N. 2015. Arc Magmatic Tempos: Gathering the Evidence. *Elements*, **11**, 91-
549 98.

550 RILEY, T.R. & KNIGHT, K.B. 2001. Age of pre-break-up Gondwana magmatism: a review. *Antarctic*
551 *Science*, **13**, 99-110.

552 RILEY, T.R., LEAT, P.T., PANKHURST, R.J. & HARRIS, C. 2001. Origins of large volume rhyolitic volcanism in
553 the Antarctic Peninsula and Patagonia by crustal melting. *Journal of Petrology*, **42**, 1043-1065.

554 RILEY, T.R., FLOWERDEW, M.J. & WHITEHOUSE, M.J. 2012. U-Pb ion-microprobe zircon geochronology
555 from the basement inliers of eastern Graham Land, Antarctic Peninsula. *Journal of the Geological*
556 *Society, London*, **169**, 381-393.

557 RILEY, T.R., CURTIS, M.L., FLOWERDEW, M.J. & WHITEHOUSE, M.J. 2016. Evolution of the Antarctic
558 Peninsula lithosphere: evidence from Mesozoic mafic rocks. *Lithos*, **244**, 59-73.

559 ROWLEY, P.D. 1990. Jones Mountains. In LEMASURIER, W.E. & THOMSON, J.W. eds. *Volcanoes of the*
560 *Antarctic Plate and southern oceans*. Washington DC: American Geophysical Union, 286-288.

561 SIDDOWAY, C.S., SASS, L.C. III & ESSER, R.P. 2005. Kinematic history of the Marie Byrd Land terrane, West
562 Antarctica: direct evidence from Cretaceous mafic dykes. In VAUGHAN, A.P.M., LEAT, P.T. &

563 PANKHURST, R.J. *eds. Terrane Processes at the Margins of Gondwana*. Geological Society, London,
564 Special Publications, 246, 417-438.

565 SCOTT, J.M., COOPER, A.F., PALIN, J.M., TULLOCH, A.J., KULA, J., JONGENS, R., SPELL, T.L. & PEARSON, N.J. 2009.
566 Tracking the influence of a continental margin on growth of a magmatic arc, Fiordland, New
567 Zealand, using thermobarometry, thermochronology, and zircon U-Pb and Hf isotopes. *Tectonics*,
568 **28**, TC6007.

569 STACEY, J.S. & KRAMERS, J.D. 1975. Approximation of terrestrial lead evolution by a two-stage model.
570 *Earth and Planetary Science Letters* **26**, 207-221.

571 STOREY, B.C., DALZIEL, I.W.D., GARRETT, S.W., GRUNOW, A.M., PANKHURST, R.J. & VENNUM, W.R. 1988. West
572 Antarctica in Gondwanaland: crustal blocks, reconstruction and break-up processes.
573 *Tectonophysics*, 155, 381-390.

574 STOREY, B.C., PANKHURST, R.J., MILLAR, I.L., DALZIEL, I.W.D. & GRUNOW, A.M. 1991. A new look at the
575 geology of Thurston Island. *In* THOMSON, M.R.A, CRAME, J.A. & THOMSON, J.W. (*eds.*) *Geological*
576 *evolution of Antarctica*. Cambridge University Press, Cambridge, 399-403.

577 VAUGHAN, A.P.M. & MILLAR, I.L. 1996. Early Cretaceous magmatism during extensional deformation
578 within the Antarctic Peninsula magmatic arc. *Journal of South American Earth Sciences*, **9**, 121-
579 129.

580 VAUGHAN, A.P.M., LEAT, P.T., DEAN, A.A. & MILLAR, I.L. 2012. Crustal thickening along the West Antarctic
581 Gondwana margin during mid-Cretaceous deformation of the Triassic intra-oceanic Dyer Arc.
582 *Lithos*, **142-143**, 130-147.

583 VEEVERS, J.J. 2012. Reconstructions before rifting and drifting reveal the geological connections
584 between Antarctica and its conjugates in Gondwanaland. *Earth Science Reviews*, **111**, 249-318.

585 WAIGHT, T.E., WEAVER, S.D. & MUIR, R.J. 1998. Mid-Cretaceous granitic magmatism during the
586 transition from subduction to extension in southern New Zealand: a chemical and tectonic
587 synthesis. *Lithos*, **45**, 469-482.

588 WHITE, C.M. & CRADDOCK, C. 1987. Compositions of igneous rocks in the Thurston Island area,
589 Antarctica: evidence for a late Palaeozoic – middle Mesozoic andinotype continental margin.
590 *Journal of Geology*, **95**, 699-709.

591 WHITEHOUSE, M.J. & KAMBER, B. 2005. Assigning dates to thin gneissic veins in high-grade
592 metamorphic terranes: a cautionary tale from Akilia, southwest Greenland. *Journal of Petrology*,
593 **46**, 291-318.

594 WIEDENBECK, M., ALLE, P., CORFU, F., GRIFFIN, W.L., MEIRER, M., OBERLI, F., VON QUADT, A., RODDICK, J.C. &
595 SPIEGEL, W. 1995. Three natural zircon standards for U-Th-Pb, Lu-Hf, trace element and REE
596 analyses. *Geostandards Newsletter*, **19**, 1-23.

597 WILLIAMS, I.S. 1998. U-Th-Pb geochronology by ion microprobe. In MCKIBBEN, M.A. & SHANKS, W.C. eds.
598 *Applications of microanalytical techniques to understanding mineralizing processes 7*, 1-35,
599 Reviews in Economic Geology.

600 WYSOCZANSKI, R.J., GIBSON, G.M. & IRELAND, T.R. 1997. Detrital zircon age patterns and provenance in
601 Late Paleozoic- Early Mesozoic New Zealand: terranes and development of the Paleo-Pacific
602 Gondwana margin. *Geology*, **25**, 939-942.

603 YAKYMCHUK, C., SIDDOWAY, C.S., FANNING, C.M., MCFADDEN, R., KORHONEN, F.J. & BROWN, M. 2013.
604 Anatectic reworking and differentiation of continental crust along the active margin of
605 Gondwana: a zircon Hf-O perspective from West Antarctica. In Harley, S.L., Fitzsimmons, I.C.W. &
606 Zhao, Y. eds. *Antarctica and supercontinent evolution*. Geological Society of London Special
607 Publication 383, doi.10.1144/SP383.7.

608 YAKYMCHUK, C., BROWN, C.R., BROWN, M., SIDDOWAY, C.S., FANNING, C.M. & KORHONEN, F.J. 2015.
609 Paleozoic evolution of western Marie Byrd Land, Antarctica. *Geological Society of America*
610 *Bulletin*, **127**, 1464-1484.

611

List of Figures

Fig. 1: Map of Antarctica showing the main crustal blocks of West Antarctica. EWM: Ellsworth-

Whitmore Mountains; HN: Haag Nunataks. (1): Northwest Palmer Land location of Mount Eissenger, Pegasus Mountains, Campbell Ridge and Sirius Cliffs; (2): Joerg Peninsula; (3): Fosdick Mountains, Marie Byrd Land.

Fig. 2: (a) Map of Thurston Island and the adjacent Eights Coast. (b) Map of Thurston Island and place names referred to in the text.

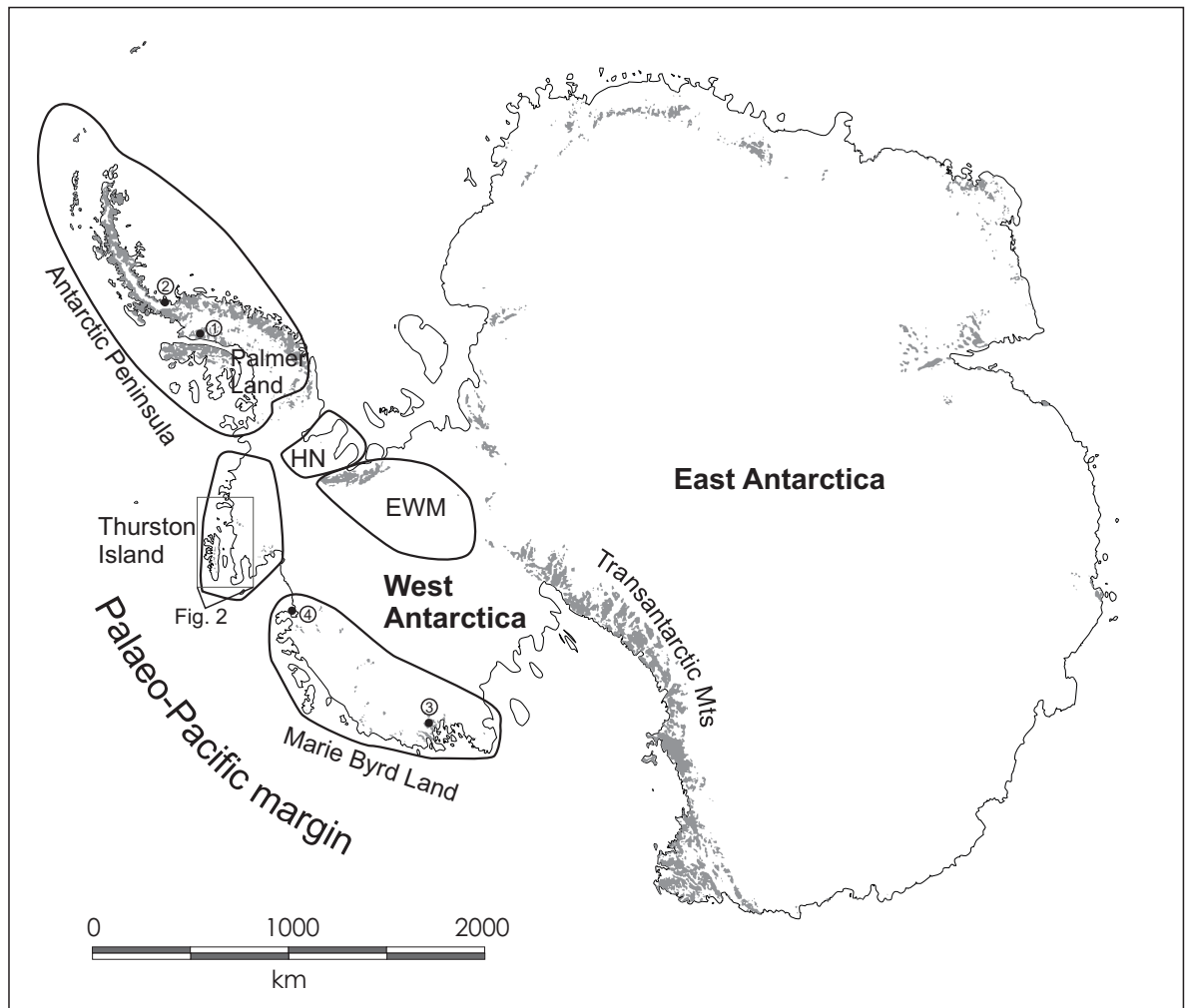
Fig. 3: Concordia diagrams for analysed zircons from the Thurston Island crustal block (a) Morgan Inlet granodiorite gneiss and Mount Bramhall diorite; (b) Mount Dowling rhyolites; (c) Hale Glacier granite and Lepley Nunatak granite.

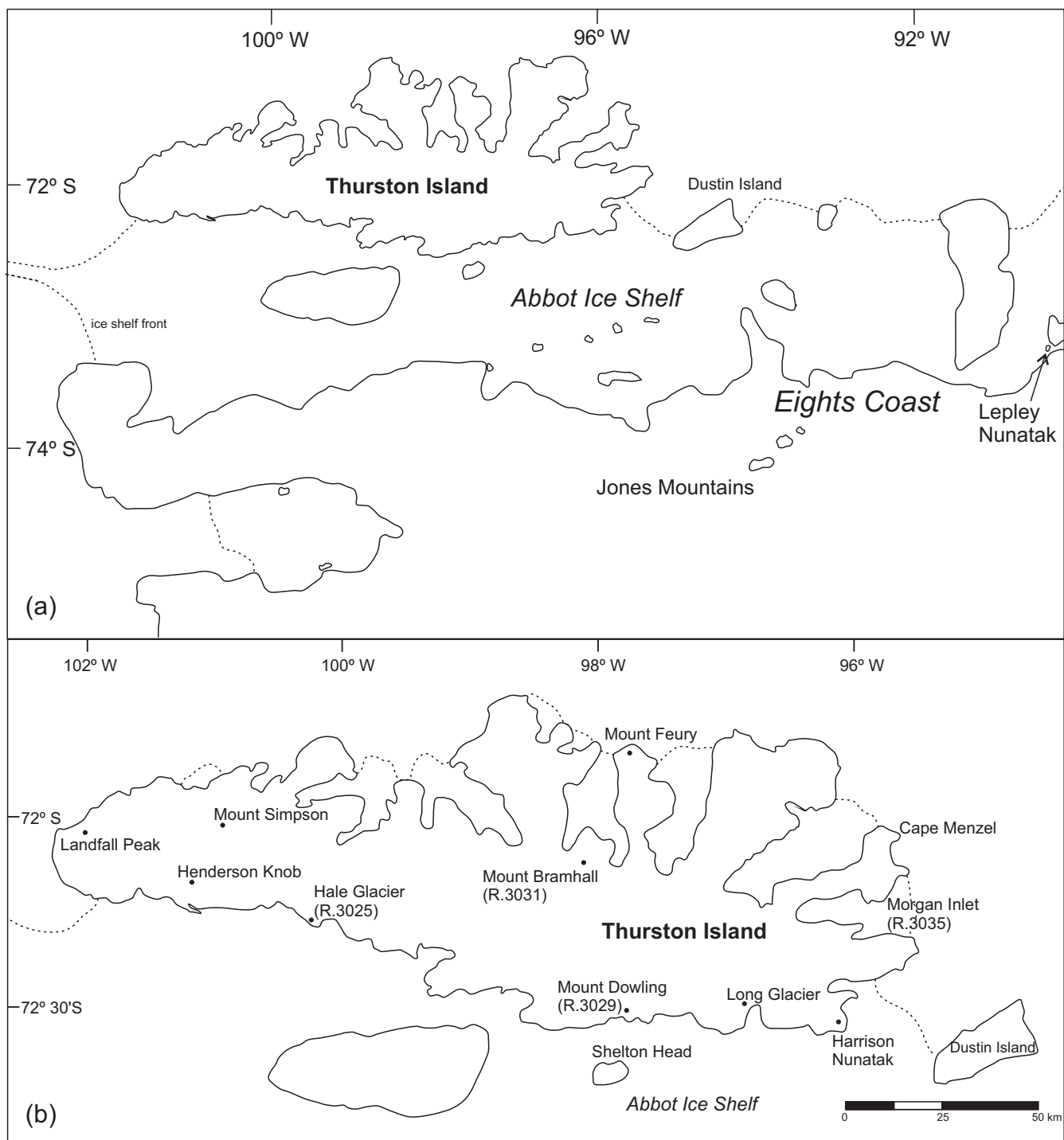
Fig. 4: Hf evolution diagram from zircon grains from sites on Thurston Island. Black diamonds: Thurston Island (this study); purple squares: Marie Byrd Land (Yakmchuk et al., 2013, 2015; Korhonen et al., 2010); olive green squares: New Zealand (Scott et al., 2009); red squares: Antarctic Peninsula (Flowerdew et al., 2006). The grey band represents the crustal evolution for the Haag Nunataks gneisses with a $^{176}\text{Lu}/^{177}\text{Hf}$ of 0.015 (Flowerdew et al., 2007).

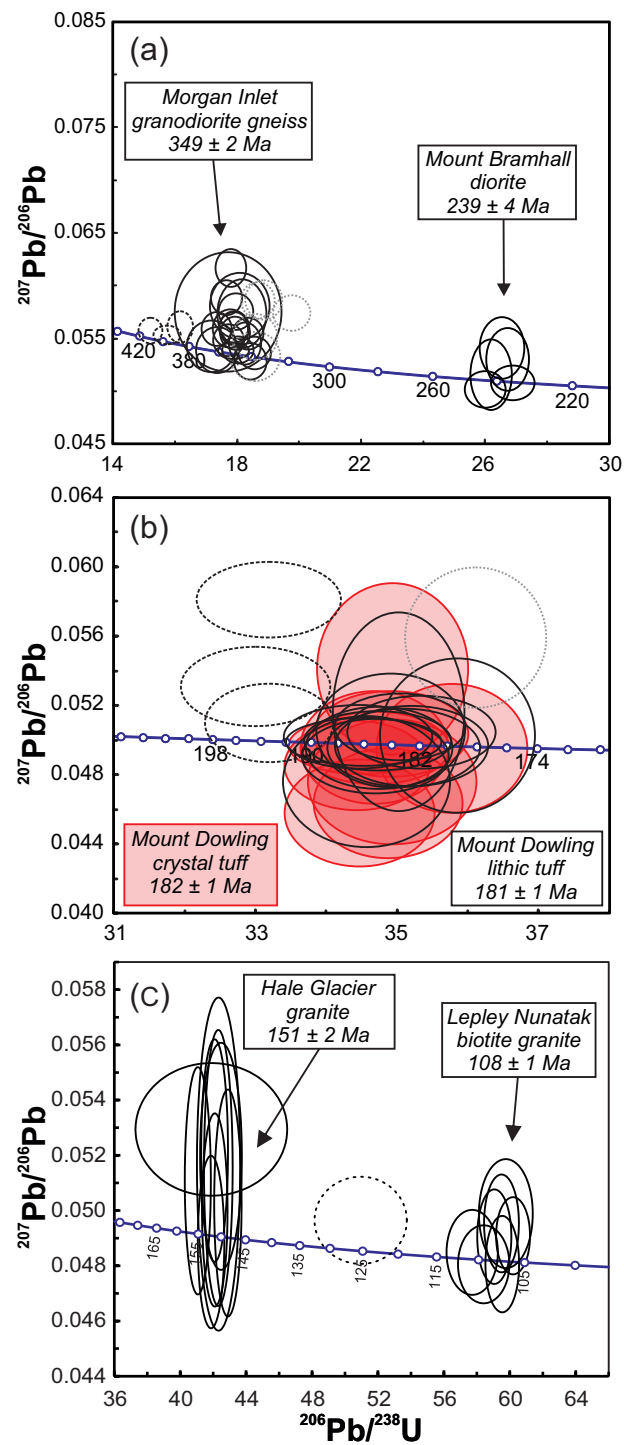
Fig. 5: Gondwana Pacific margin reconstruction at ~185 Ma (Veevers 2012). The dashed line reconstruction position of Thurston Island is from Elliot et al. (2016). E.Ant: East Antarctica; S.Am: South America; PAT: Patagonia; S.Afr: South Africa; FI: Falkland Islands; EWM: Ellsworth-Whitmore Mountains; AP: Antarctic Peninsula; AI: Alexander Island; CR: Chatham Rise; EMBL: Eastern Marie Byrd Land; TI: Thurston Island.

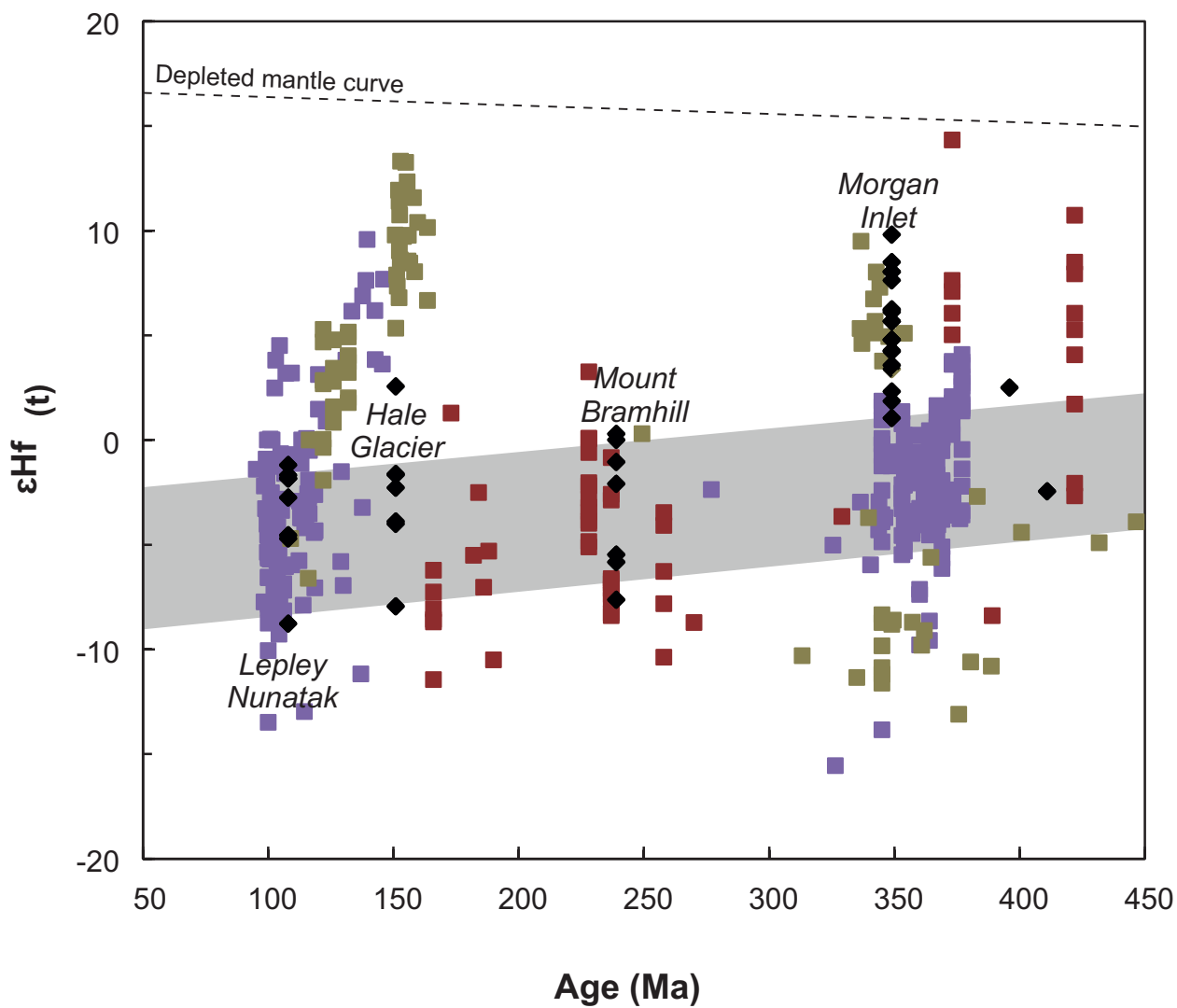
Fig. 6: $^{87}\text{Sr}/^{86}\text{Sr}$ vs. ϵNd for Early Jurassic silicic volcanic rocks from Mount Dowling on Thurston Island in comparison to rhyolitic volcanic rocks from the V1 episode of the Chon Aike Province (Marifil, Mount Poster and Brennecke formations), Lebombo volcanic rocks, Transantarctic Mountains (Riley et al., 2001).

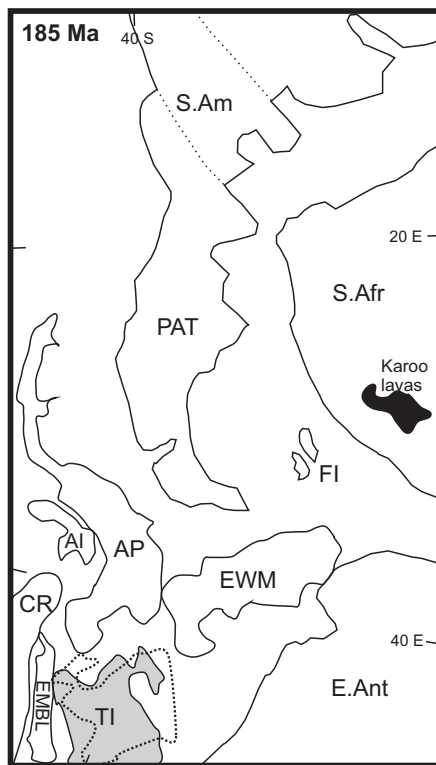
Supplementary Figure 1: Cathodoluminescence images of analysed zircon grains from sites on Thurston Island. Circles indicate the position of analysis (U-Pb (red) and Hf (blue) analyses). (a) Morgan Inlet; (b) Mount Bramhall; (c) Mount Dowling R.3029.1; (d) Mount Dowling R.3029.3 (e) Hale Glacier; (f) Lepley Nunatak.

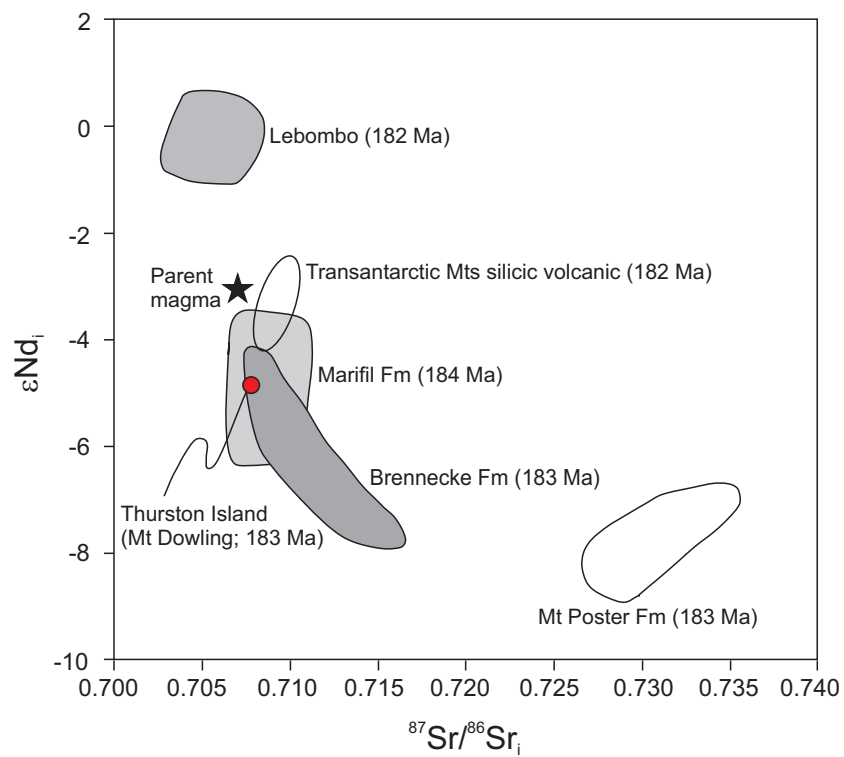




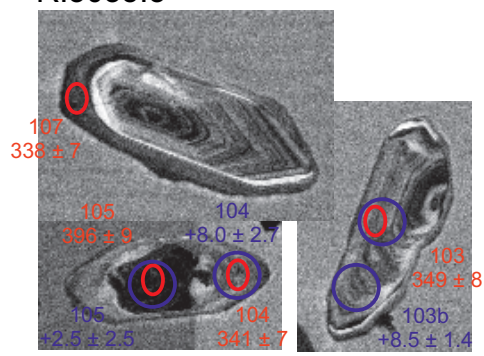




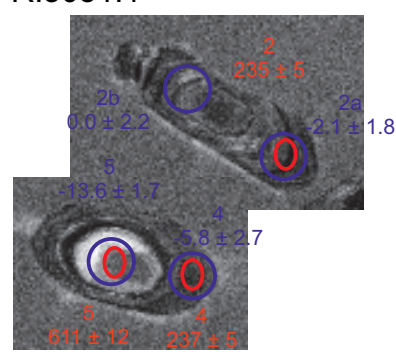




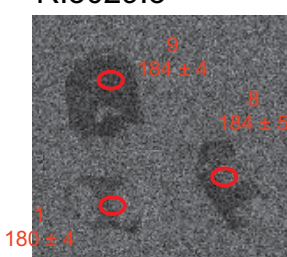
a) Morgan Inlet gneiss
R.3035.3



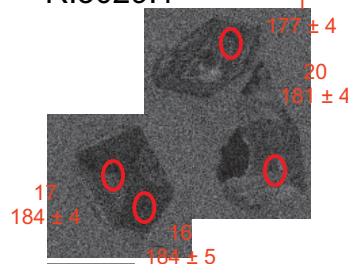
b) Mount Bramhall diorite
R.3031.1



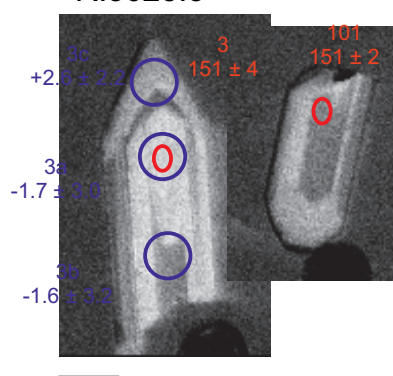
c) Mount Dowling crystal tuff
R.3029.3



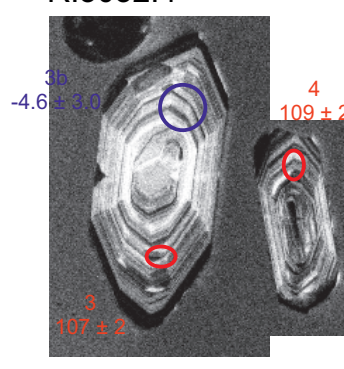
d) Mount Dowling lithic tuff
R.3029.1



e) Hale Glacier
R.3025.3



f) Lepley Nunatak
R.3032.4



Supplementary Figure 1. Representative CL images of analysed zircons showing the location of U-Pb (red) and Hf (blue) analyses. Age and ϵ_{Hf} values are quoted with 2σ uncertainties

Table 1: U-Pb zircon ion microprobe analyses

spot id	zone	Concentrations (ppm)				isotope ratios				Ages (Ma)					
		U	Th	Pb	Th/U	$f_{206}\%^1$	$^{238}\text{U}/^{206}\text{Pb}$	$\pm\sigma$ (%)	$^{207}\text{Pb}/^{206}\text{Pb}$	$\pm\sigma$ (%)	$^{207}\text{Pb}/^{206}\text{Pb}$	$\pm\sigma$	$^{206}\text{Pb}/^{238}\text{U}$	$\pm\sigma$	
R.3035.3. Granodiorite gneiss, Morgan Inlet															
7.1*	Pb loss	186.25	8.57	8.10	0.05	0.59	19.757	1.24	0.0574	1.24	507.8	52.1	318.3	3.9	
6.1*	Pb loss	160.67	43.88	7.32	0.27	0.70	18.852	1.28	0.0587	1.28	554.2	47.0	333.2	4.2	
14.1*	Pb loss	246.71	87.27	11.35	0.35	0.68	18.674	1.18	0.0586	1.18	551.6	38.6	336.3	3.9	
4.1*		229.39	67.35	10.60	0.29	0.01	18.591	1.79	0.0533	1.79	341.8	42.6	337.7	6.0	
2.1*		1476.34	75.28	0.25	0.05	68.2	18.585	1.58	0.0552	1.58	419.6	22.5	337.8	5.2	
107	outer	318.89	109.20	19.99	0.34	{0.15}	18.574	1.14	0.0537	1.15	356.8	25.9	338.0	3.7	
104		224.99	24.48	13.32	0.11	{0.18}	18.417	1.14	0.0528	1.30	319.8	29.3	340.9	3.8	
8.1*		315.82	89.03	14.78	0.28	0.27	18.361	1.13	0.0555	1.13	431.1	35.0	341.9	3.8	
102		241.52	95.86	15.72	0.40	{0.03}	18.256	1.14	0.0545	1.48	391.5	32.8	343.8	3.8	
1.1*		231.01	54.03	0.50	0.23	10.9	18.162	1.78	0.0573	2.36	504.9	52.9	345.5	6.1	
11.1*		198.30	9.18	9.41	0.05	0.58	18.099	2.20	0.0581	2.20	531.7	42.1	346.7	7.5	
103		383.19	187.06	25.86	0.49	{0.08}	18.024	1.13	0.0539	1.00	368.5	22.4	348.1	3.8	
17.1*		227.63	31.73	10.88	0.14	0.50	17.967	1.26	0.0575	1.26	510.7	40.6	349.2	4.3	
10.1*		277.17	82.65	13.27	0.30	0.25	17.942	1.14	0.0555	1.14	433.3	36.0	349.6	3.9	
15.1*		328.41	108.82	15.75	0.33	0.31	17.909	1.13	0.0559	1.13	450.2	42.4	350.3	3.9	
13.1*		448.32	214.33	21.51	0.48	0.32	17.905	1.08	0.0560	1.08	454.0	29.5	350.3	3.7	
101	outer	1070.45	70.81	64.40	0.07	{0.14}	17.876	1.13	0.0538	0.60	363.8	13.4	350.9	3.9	
2b.1*		233.43	54.15	11.26	0.23	1.02	17.815	1.16	0.0617	1.16	662.4	34.8	352.1	4.0	
20.1*		333.29	153.10	16.11	0.46	0.29	17.777	1.29	0.0559	1.29	449.0	35.2	352.8	4.5	
9.1*		696.28	5.15	33.74	0.01	0.15	17.729	1.12	0.0548	1.12	404.1	23.4	353.7	3.9	
19.1*		417.54	190.29	20.30	0.46	0.66	17.667	1.18	0.0589	1.18	562.3	29.6	354.9	4.1	
3.1*	inherited	526.00	30.42	26.05	0.06	0.02	17.346	1.63	0.0539	1.63	368.4	28.7	361.3	5.8	
18.1*	inherited	269.68	88.55	13.36	0.33	0.27	17.344	1.17	0.0559	1.17	449.8	37.5	361.4	4.2	
21.1*	inherited	414.98	171.89	20.75	0.41	0.06	17.180	1.83	0.0543	1.83	383.1	30.0	364.7	6.6	
16.1*	core	568.16	241.81	30.18	0.43	0.21	16.174	1.05	0.0561	1.05	454.7	24.7	386.7	4.0	
105	core	699.60	302.62	52.84	0.43	0.11	15.761	1.13	0.0553	0.66	424.0	14.9	396.2	4.3	
5.1*	core	201.10	41.18	16.67	0.20	0.15	10.361	1.15	0.0610	1.15	638.1	29.0	594.0	6.7	
106	core	55.83	54.55	13.29	0.98	{0.21}	5.839	1.12	0.0753	1.45	1077.6	28.9	1019.1	10.6	
R.3031.1. Coarsely crystalline biotite-hornblende granodiorite, Mount Bramhall															
2		267.27	184.84	12.76	0.69	{0.10}	26.890	1.03	0.0508	1.35	230.4	30.8	235.4	2.4	
4		269.60	72.21	11.55	0.27	{0.19}	26.720	1.06	0.0530	2.27	328.4	50.6	236.8	2.5	
8		156.22	122.21	7.73	0.78	{0.36}	26.530	1.08	0.0541	2.18	375.7	48.3	238.5	2.5	
7		285.72	179.40	13.70	0.63	{0.24}	26.167	1.05	0.0516	2.66	266.2	60.0	241.8	2.5	
3		397.34	171.19	18.24	0.43	{0.11}	25.982	1.05	0.0502	1.36	202.0	31.4	243.5	2.5	
1	core	379.44	224.42	31.38	0.59	{0.12}	15.207	1.02	0.0557	0.89	441.2	19.8	410.6	4.1	
5	core	114.08	269.55	20.40	2.36	{0.12}	10.064	1.03	0.0610	1.50	639.9	32.0	610.7	6.0	
6	core	446.34	194.11	86.83	0.43	{0.03}	6.219	1.02	0.0733	0.62	1023.4	12.5	961.2	9.1	
R.3029.3. Rhyolite tuff, Mount Dowling															
3 Pb loss		269.97	153.99	9.21	0.57	0.41	35.772	1.23	0.0496	3.02	174.2	72.0	177.0	2.1	
1		143.31	73.90	4.87	0.52	1.12	34.944	1.26	0.0541	3.71	375.3	85.8	179.9	2.2	
5		158.92	124.32	5.80	0.78	0.63	34.934	1.39	0.0476	3.11	78.2	75.6	180.8	2.5	
7		379.60	261.10	13.70	0.69	0.38	34.923	1.28	0.0504	1.98	212.0	46.5	181.3	2.3	
10		212.61	158.64	7.70	0.75	0.50	34.870	1.23	0.0463	2.77	15.6	68.0	181.4	2.2	
6		206.62	113.43	7.21	0.55	0.40	34.686	1.23	0.0496	2.67	175.2	63.6	182.5	2.2	
2		586.79	417.03	21.40	0.71	0.35	34.694	1.22	0.0495	1.73	173.9	41.0	182.6	2.2	
8		211.36	150.50	7.67	0.71	0.30	34.475	1.24	0.0458	2.77	-12.6	68.3	183.8	2.3	
4		1124.40	989.07	43.21	0.88	0.12	34.502	1.22	0.0497	1.34	179.2	31.6	184.0	2.2	
9		433.40	258.44	15.36	0.60	0.30	34.431	1.22	0.0485	2.16	125.5	51.7	184.0	2.2	
R.3029.1. Rhyolite tuff, Mount Dowling															
2 Pb loss		176.82	94.55	5.92	0.53	0.76	36.114	1.14	0.0559	2.95	448.5	66.8	174.8	1.9	
1 Pb loss		329.27	142.74	10.88	0.43	0.34	35.856	1.23	0.0502	3.63	205.8	86.6	176.7	2.2	
9		525.12	508.96	20.15	0.97	0.33	35.348	1.21	0.0504	1.69	214.9	39.5	179.3	2.1	
10		487.09	247.57	16.64	0.51	0.26	35.213	1.25	0.0496	1.90	177.7	44.8	180.1	2.2	
18		475.20	401.97	17.89	0.85	0.23	35.096	1.25	0.0495	1.86	173.4	43.9	180.7	2.2	
3		633.91	900.10	27.11	1.42	0.29	35.040	1.08	0.0508	1.53	230.8	35.7	180.9	1.9	
8		500.40	267.40	17.40	0.53	0.30	35.028	1.09	0.0517	4.40	274.1	104.1	180.9	1.9	
20		263.29	228.76	9.84	0.87	0.62	34.899	1.22	0.0505	2.68	218.4	63.3	181.0	2.2	
15		425.10	297.70	15.47	0.70	0.40	34.740	1.22	0.0496	1.95	175.5	46.2	182.2	2.2	
13		839.59	604.86	30.72	0.72	0.24	34.724	1.22	0.0499	1.41	192.4	33.2	182.6	2.2	
19		510.85	391.44	18.92	0.77	0.22	34.710	1.22	0.0491	1.77	150.6	42.1	182.7	2.2	
12		159.02	98.04	5.64	0.62	0.44	34.564	1.40	0.0476	3.24	79.1	78.8	183.1	2.5	
16		1254.25	1106.58	48.01	0.88	0.16	34.539	1.29	0.0499	1.15	190.0	27.1	183.7	2.3	
17		868.59	1040.99	35.97	1.20	0.05	34.453	1.23	0.0501	1.49	201.8	35.1	184.4	2.2	
5	core	2765.23	2545.65	110.85	0.92	1.02	33.188	1.25	0.0581	1.52	534.4	33.7	189.4	2.3	
7	core	466.55	285.92	17.41	0.61	0.20	33.203	1.12	0.0510	1.80	241.6	42.1	190.9	2.1	
6	core	853.99	584.30	32.68	0.68	0.48	33.004	1.31	0.0531	1.76	334.8	40.3	191.5	2.5	
14	core	548.68	238.25	36.79	0.43	0.90	17.240	1.22	0.0534	1.18	344.9	27.0	360.3	4.3	
11	core	977.89	164.16	148.86	0.17	0.10	7.377	1.22	0.0718	0.51	980.4	10.4	818.8	9.4	
4	core	1202.33	1888.64	418.74	1.57	0.06	4.669	2.43	0.1580	1.05	2434.2	17.9	1250.3	27.7	

R.3025.3. Coarsely crystalline granite, Hale Glacier

104		64.30	52.08	1.97	0.81 {0.70}	42.894	0.79	0.0503	3.34	207.6	75.7	148.6	1.2
2		88.12	85.32	2.83	0.97 {0.65}	42.475	1.22	0.0520	3.23	283.8	72.3	150.0	1.8
3		71.49	66.38	2.28	0.93 {2.34}	42.327	1.27	0.0517	4.77	271.3	105.8	150.5	1.9
101		44.11	26.81	1.30	0.61 {0.67}	42.312	0.84	0.0515	3.96	265.1	88.5	150.6	1.3
103		112.91	93.90	3.55	0.83 {0.22}	42.098	0.75	0.0500	2.86	196.0	65.1	151.3	1.1
106		70.29	52.80	2.17	0.75 {0.55}	42.086	0.79	0.0522	3.16	293.0	70.5	151.4	1.2
102		106.96	88.79	3.38	0.83 {0.15}	41.872	0.79	0.0489	2.61	141.1	60.2	152.1	1.2
105		63.35	43.21	1.97	0.68 {0.29}	41.069	0.79	0.0511	3.29	244.3	74.1	155.1	1.2

R.3032.4. Coarsely crystalline biotite granite, Lepley Nunatak

103		763.93	243.28	14.62	0.32 {0.09}	60.197	0.70	0.0491	1.16	152.0	27.0	106.2	0.7
3		459.48	143.02	8.90	0.31 {0.26}	59.759	1.12	0.0499	1.62	189.8	37.2	107.0	1.2
101		677.13	213.69	13.11	0.32 {0.01}	59.541	0.70	0.0481	1.48	102.2	34.7	107.4	0.7
102		481.59	151.43	9.35	0.31 {0.09}	59.494	0.73	0.0495	1.46	173.2	33.7	107.5	0.8
105		501.14	89.14	9.34	0.18 0.17	59.059	0.72	0.0491	1.43	86.0	40.1	108.1	0.8
4		860.50	231.19	16.80	0.27 {0.13}	58.413	1.09	0.0481	1.20	101.9	28.1	109.4	1.2
2		904.97	312.00	18.30	0.34 {0.20}	57.717	1.10	0.0485	1.30	123.0	30.3	110.7	1.2
104	core	517.28	187.59	11.92	0.36 {0.07}	50.951	2.24	0.0496	1.30	178.5	30.0	125.3	2.8
106	core	595.18	146.09	15.89	0.25 {0.06}	41.891	4.49	0.0529	1.85	326.2	41.5	152.1	6.7
2	core	286.18	101.03	19.46	0.35 {0.07}	17.345	1.07	0.0570	1.75	492.5	38.1	361.3	3.8

Table 2: Lu-Hf isotope analyses

spot # ¹	age ²	¹⁷⁶ Lu/ ¹⁷⁷ Hf	¹⁷⁶ Yb/ ¹⁷⁷ Hf	¹⁷⁶ Hf/ ¹⁷⁷ Hf ³	±2σ	εHf _t ⁴	±2σ	t _{DM} ⁵
<i>R.3035.3 Thurston Island - Morgan Inlet (n = 23)</i>								
6.1	349	0.0007	0.0217	0.282666	0.000075	3.4	2.6	787
8.1	349	0.0007	0.0209	0.282743	0.000051	6.1	1.8	679
10.1	349	0.0007	0.0222	0.282706	0.000062	4.8	2.2	732
12.1	349	0.0009	0.0276	0.282637	0.000072	2.3	2.6	833
13.2	349	0.0008	0.0232	0.282731	0.000057	5.7	2.0	697
15.1	349	0.0006	0.0165	0.282704	0.000081	4.8	2.9	731
16.1	349	0.0011	0.0372	0.282602	0.000060	1.0	2.1	886
18.1	349	0.0006	0.0198	0.282746	0.000062	6.2	2.2	674
17.1	349	0.0008	0.0246	0.282690	0.000053	4.2	1.9	755
1.1a	349	0.0007	0.0173	0.282623	0.000071	1.9	2.5	847
1.1b	349	0.0008	0.0243	0.282798	0.000078	8.0	2.8	605
1.1c	349	0.0009	0.0301	0.282692	0.000052	4.3	1.8	755
2.1	349	0.0009	0.0296	0.282732	0.000047	5.7	1.7	699
1	349	0.0006	0.0168	0.282670	0.000084	3.6	3.0	779
102a	349	0.0004	0.0104	0.282743	0.000048	6.2	1.7	674
102b	349	0.0007	0.0190	0.282785	0.000034	7.6	1.2	620
103a	349	0.0010	0.0276	0.282849	0.000034	9.8	1.2	535
103b	349	0.0007	0.0185	0.282810	0.000041	8.5	1.4	585
104	349	0.0006	0.0145	0.282796	0.000077	8.0	2.7	602
105	396	0.0021	0.0718	0.282622	0.000070	2.5	2.5	881
5.1 core	593	0.0006	0.0307	0.282454	0.000081	1.2	2.9	1081
<i>R.3031.1 Thurston Island - Mount Bramhall diorite (n=10)</i>								
7	239	0.0011	0.0300	0.282648	0.000104	0.3	3.7	820
8	239	0.0010	0.0321	0.282610	0.000112	-1.0	4.0	873
3a	239	0.0006	0.0185	0.282422	0.000113	-7.6	4.0	1125
3b	239	0.0011	0.0365	0.282485	0.000095	-5.5	3.4	1051
2a	239	0.0008	0.0272	0.282579	0.000050	-2.1	1.8	910
2b	239	0.0010	0.0335	0.282639	0.000061	0.0	2.2	830
4	239	0.0004	0.0121	0.282472	0.000075	-5.8	2.7	1050
6	1023	0.0011	0.0351	0.282456	0.000095	10.5	3.4	1092
1	411	0.0011	0.0450	0.282466	0.000104	-2.5	3.7	1079
5	611	0.0009	0.0305	0.282025	0.000048	-13.6	1.7	1684
<i>R.3025.1 Thurston Island - Hale Glacier (n = 7)</i>								
1a	151	0.0009	0.0275	0.282468	0.000099	-7.9	3.5	1068
1b	151	0.0009	0.0371	0.282629	0.000063	-2.3	2.2	845
2a	151	0.0010	0.0349	0.282583	0.000068	-3.9	2.4	909
2b	151	0.0010	0.0356	0.282580	0.000051	-4.0	1.8	914
3a	151	0.0011	0.0333	0.282646	0.000085	-1.7	3.0	823
3b	151	0.0009	0.0288	0.282647	0.000090	-1.6	3.2	817
3c	151	0.0005	0.0181	0.282764	0.000063	2.6	2.2	647
<i>R.3032.4 Thurston Island - Lepley Nunatak granite (n = 9)</i>								
1a	108	0.0014	0.0429	0.282587	0.000121	-4.7	4.3	914
1b	108	0.0013	0.0449	0.282672	0.000090	-1.7	3.2	791
3b	108	0.0009	0.0303	0.282590	0.000089	-4.6	3.2	898
4a	108	0.0011	0.0434	0.282642	0.000084	-2.7	3.0	831
4b	108	0.0014	0.0532	0.282686	0.000065	-1.2	2.3	773
4c	108	0.0013	0.0494	0.282472	0.000082	-8.8	2.9	1074
4d	108	0.0015	0.0648	0.282668	0.000059	-1.8	2.1	801
4e	108	0.0015	0.0688	0.282668	0.000051	-1.8	1.8	802

1. Spot identification number.

2. Age sample or portion of grain analysed.

3. Values using a modified Thirlwall & Walder (1995) doping method for correcting the interfering ^{176}Yb (Flowerdew et al. 2006).
4. Calculated using Lu decay constant of 1.865×10^{-11} (Scherer et al. 2001), $^{176}\text{Hf}/^{177}\text{Hf}$ and $^{176}\text{Lu}/^{177}\text{Hf}$ (CHUR) values of 0.282785 and 0.0336, respectively (Bouvier et al. 2008).
5. Depleted mantle model ages were calculated using present day $^{176}\text{Hf}/^{177}\text{Hf}$ and $^{176}\text{Lu}/^{177}\text{Hf}$ values of 0.28325 and 0.0384, respectively (Griffin et al. 2004). All references in Flowerdew et al. (2006)

